

Ab initio study on fracture toughness of $\text{Ti}_{0.75}\text{X}_{0.25}\text{C}$ ceramics

Kuiying Chen · Mariusz Bielawski

Received: 24 April 2007 / Accepted: 11 June 2007 / Published online: 31 July 2007
© Springer Science+Business Media, LLC 2007

Abstract Ab initio density functional theory calculations have been performed to evaluate the fracture toughness for selected $\text{Ti}_{0.75}\text{X}_{0.25}\text{C}$ ceramics ($X = \text{Ta}, \text{W}, \text{Mo}, \text{Nb}$ and V). The calculated Young's modulus E , surface energy γ and fracture toughness K_{IC} of pure TiC are in a good agreement with experimental data and other theoretical calculations. The results for $\text{Ti}_{0.75}\text{X}_{0.25}\text{C}$ system show that alloying additions increase Young's modulus, and all but vanadium increase surface energy. It was observed that tungsten has the most significant effect on increasing Young's modulus, while tantalum on increasing surface energy of the $\text{Ti}_{0.75}\text{X}_{0.25}\text{C}$ system. Surface energy plays a dominated role in determining the trend of fracture toughness. Overall, tantalum and tungsten are the most effective alloying elements in increasing the fracture toughness of $\text{Ti}_{0.75}\text{X}_{0.25}\text{C}$ ceramics.

Introduction

Particulate dry erosion is one of the modes of material degradation that can significantly impact component life and system safety in aerospace system. To extend the service life of aircraft engines operated in desert areas, attempts were made to develop advanced erosion-resistant (ER) coatings for compressor components of gas turbine engines [1–4]. Despite these efforts, only TiN-based

coatings are currently approved for aerospace applications. These coatings can, however, extend the service life of compressor blades by no more than a factor of three. To achieve better performance, new erosion materials and new design methods need to be developed. In the early stage of erosion coating development, material hardness was considered to be a key factor in increasing the erosion resistance of protective coatings. Many of extremely hard coating materials, such as ceramics, failed to provide an expected performance. Erosion theories developed in the 1970s clearly demonstrated that both hardness and fracture toughness of materials were critical properties in determining erosion resistance of brittle ceramic coatings [5, 6]. However, the existing analytical solutions due to the complexity of the erosion process and the restrictive assumptions used to derive these models could only give a general direction, and have a limited value as design tools in ER coating development. In addition, the traditional methods of developing protective coatings through trial-and-error experimentation are time consuming and costly.

To speed up the experimental development, extensive modeling and simulation efforts are required. However, to get meaningful results, the models need to be populated with actual materials and engineering data. The latter is not easily available for most of thin film materials. Advanced erosion-resistant coatings are produced using either physical or chemical vapor deposition (PVD or CVD) methods. These technologies can produce complex coatings systems consisting of many layers of different materials, typically nitrides or carbides of transition metals, at a nano scale. Although coating hardness can be easily determined using depth sensing indentation techniques, the intrinsic materials properties such as fracture toughness are virtually unknown. Therefore, developing a computational method that could allow an evaluation of fracture toughness for

K. Chen (✉) · M. Bielawski
Structures and Materials Performance Laboratory, Institute for
Aerospace Research, National Research Council Canada,
Montreal Road M-17, Ottawa, ON, Canada K1A 0R6
e-mail: kuiying.chen@nrc-cnrc.gc.ca

new coating materials would benefit both experimental and modeling efforts. To our knowledge, there are neither theoretical calculations nor experimental measurements on fracture toughness for the $\text{Ti}_{0.75}\text{X}_{0.25}\text{C}$ systems. To this end, we make the first attempt to evaluate fracture toughness of TiC-based ceramics by performing ab initio density functional theory (DFT) calculations.

Calculation methodology

The Vienna ab initio simulation package (VASP) [7, 8] using projector augmented wave (PAW) method [9] based on density functional theory with the generalized-gradient approximation (GGA) [10] was utilized to calculate the elastic modulus and surface energy. Figure 1 shows the unit cell model of $\text{Ti}_{0.75}\text{X}_{0.25}\text{C}$ ceramic for modulus calculations. An eight-atoms cubic unit cell with B1 structure was created. The open circles represent C atoms, the solid black circles represent the Ti atoms, while the gray circle in the center represents a single alloying atom X replacing one Ti atom. Thus, the composition ratio of the model is $\text{Ti}:\text{X}:\text{C} = 0.75:0.25:1$. The selected alloying elements for this study were Ta, W, Nb, Mo and V. The integration in the Brillion zone of ab initio calculations was done by using Monkhorst Pack $8 \times 8 \times 8$ k-points for moduli calculations and $9 \times 9 \times 3$ k-points for surface energy evaluations. The planewave cutoff energies were ~ 450 eV, and the convergence of the calculations was within 1–2 meV. The maximum strain used in the total energy fitting to derive elastic moduli was within 1%. The unit cell model was fully relaxed during the calculation.

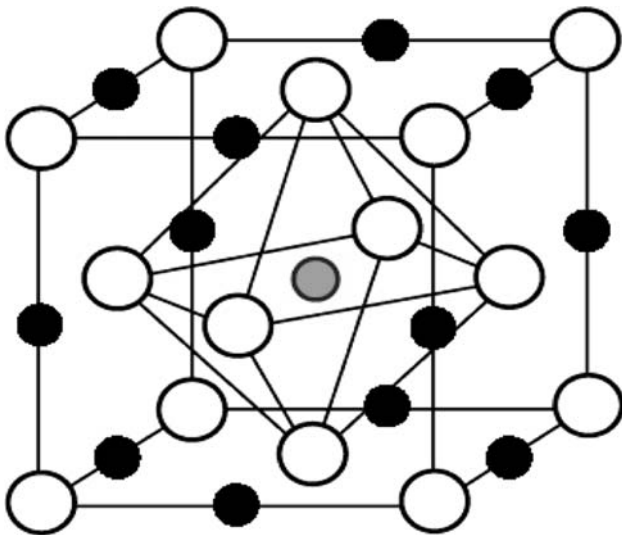


Fig. 1 The unit cell of $\text{Ti}_{0.75}\text{X}_{0.25}\text{C}$ for elastic modulus calculations. The open circles represent C atoms, while solid black circles Ti atoms, and the gray circle indicates alloying atom X (= Ta, W, Nb, Mo and V)

The elastic properties of these alloys were determined from the calculated total energy E_{tot} . The bulk modulus B can be derived directly from the second derivative of the total energy E_{tot} as a function of the volume V_0 :

$$B = V \frac{d^2 E_{\text{tot}}}{dV^2} \Big|_{V=V_0} \quad (1)$$

For cubic symmetry systems (B1), there are three independent elastic coefficients, C_{11} , C_{12} and C_{44} . The bulk modulus B is related to these two elastic coefficients C_{11} and C_{12} by:

$$B = \frac{C_{11} + 2C_{12}}{3} \quad (2)$$

In this study, C_{11} , C_{12} and C_{44} were determined by employing suitable lattice distortions represented by a strain tensor e , such that a new lattice vector r' in the distorted lattice yields $r' = (I + \varepsilon)r$, where I is the unit matrix. Furthermore, the total energy per unit cell volume and the lattice distortion e can be connected by a strain energy density $U(e)$. The tetragonal shear modulus $C' = 1/2(C_{11} - C_{12})$ can be determined by a tetragonal distortion represented by e in the [001] direction. The strain energy density $U_{\text{tet}}(e)$ for a tetragonal distortion is defined and calculated as:

$$U_{\text{tet}}(e) = \frac{3}{4} e^2 (C_{11} - C_{12}) \quad (3)$$

The second derivative of $U_{\text{tet}}(e)$ relative to e can then be derived as follows:

$$\frac{\partial^2 U_{\text{tet}}}{\partial e^2} = \frac{3}{2} (C_{11} - C_{12}) \quad (4)$$

U_{tet} can be obtained from the total energy calculations per unit cell as a function of the distortion e . Combining Eqs. 1 and 4, the elastic constants C_{11} and C_{12} were determined. Similarly, the trigonal shear constant C_{44} was calculated from a trigonal distortion. The strain energy density U_{tri} for the trigonal distortion is given by

$$U_{\text{tri}} = 2e^2 C_{44} \quad (5)$$

The value of C_{44} is obtained from the second derivative of U_{tri} relative to e

$$\frac{\partial^2 U_{\text{tri}}}{\partial e^2} = 4C_{44} \quad (6)$$

Since C_{11} , C_{12} and C_{44} comprise a complete set of elastic constants for a cubic system, the shear modulus G , Young's modulus E can be calculated from the following relations:

$$G = \frac{3C_{44} + C_{11} - C_{12}}{5} \tag{7}$$

$$E = \frac{9BG}{3B + G} \tag{8}$$

To calculate surface energy γ , a series of slab models with different thickness were generated, Fig. 2. It is observed that the calculated surface energy will converge to a stable value if the slab thickness in the model reaches a critical value. In present calculations, the critical thickness of 11 layers is enough to achieve the convergence and stable surface energy. The surface energies for the TiC and Ti_{0.75}X_{0.25}C ceramics are defined and calculated using Boettger formula [11] for (001) orientation after the relaxations

$$\gamma = (E_{\text{slab}}^N - N\Delta E)/2 \tag{9}$$

where E_{slab}^N is the total energy of an N -layer slab, and ΔE the incremental energy determined by $(E_{\text{slab}}^N - E_{\text{slab}}^{N-2})/2$. In order to prevent the interactions between the slab and its periodic images, a vacuum region at least 10 Å was

included in the supercell, Fig. 2. Fracture toughness K_{IC} is the intrinsic material property, interpreted as a critical stress intensity factor that can be calculated from the following formula [12]:

$$K_{\text{IC}} = \sqrt{4\gamma E} \tag{10}$$

where the surface energy γ and Young’s modulus E are obtained from ab initio calculations described previously.

Results and discussions

Table 1 lists the calculated Young’s modulus E , surface energy γ and fracture toughness K_{IC} for pure TiC together with experimental measurements and other density functional theory calculations. It is found that the calculated E , γ and K_{IC} values for pure TiC are in a good agreement with experimental observations [13–15] and other DFT calculations [16–18]. Table 2 presents the calculated Young’s modulus E , surface energy γ and fracture toughness K_{IC} for Ti_{0.75}X_{0.25}C systems. Figure 3 indicates that alloying additions increase Young’s moduli E , with W achieving the best effect by ~16%. It was suggested that there is a correlation between hardness H and Young’s modulus E , i.e., the larger the Young’s modulus, the higher the hardness of material [19]. As the high hardness is one key property required to achieve better performance for erosion-resistant coatings, alloying additions that increase the Young’s modulus, such as, W and Mo, will be considered as potential candidates for coating applications. In addition,

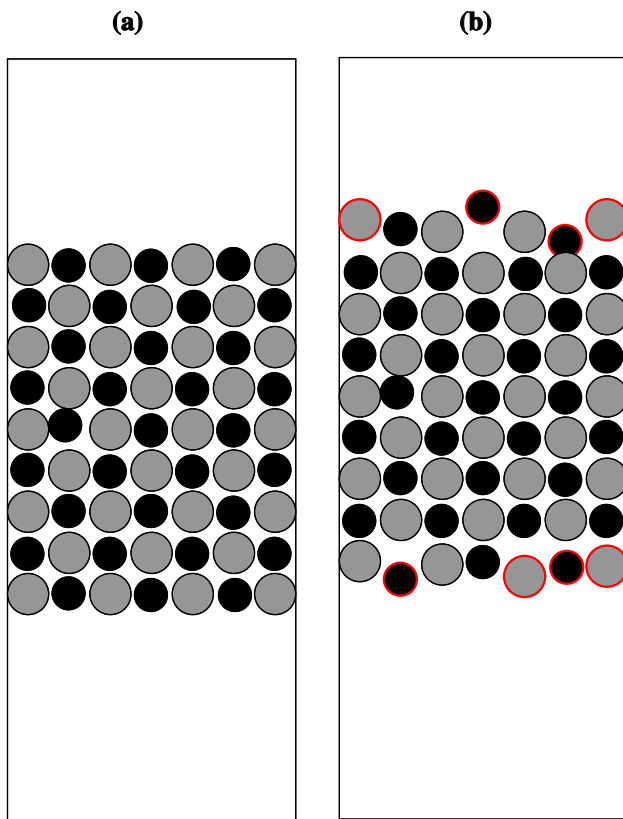


Fig. 2 Schematic diagram of a slab geometry model for surface energy calculations for TiC-based ceramics. (a) Slab model with vacuum regions before relaxation; (b) the same slab model after relaxation

Table 1 The calculated and experimental data of Young’s modulus E , (001) surface energy γ and fracture toughness K_{IC} for TiC

TiC	Present DFT calculations	Other DFT data	Experimental data
E (GPa)	429	415 [16]	448 [15]
γ (J/m ²)	1.69	1.71 [17] 1.67 [18]	–
K_{IC} (MPa m ^{1/2})	1.71	–	1.70 [14] 1.55 [13]

Table 2 Calculated Young’s modulus E , (001) surface energy γ and fracture toughness K_{IC} for Ti_{0.75}X_{0.25}C

Ti _{0.75} X _{0.25} C	TiC	X = Ta	X = W	X = Nb	X = Mo	X = V
E (GPa)	429	477	499	466	482	463
γ (J/m ²)	1.69	2.55	2.43	2.13	1.93	1.67
K_{IC} (MPa m ^{1/2})	1.71	2.2	2.2	2.01	1.93	1.76

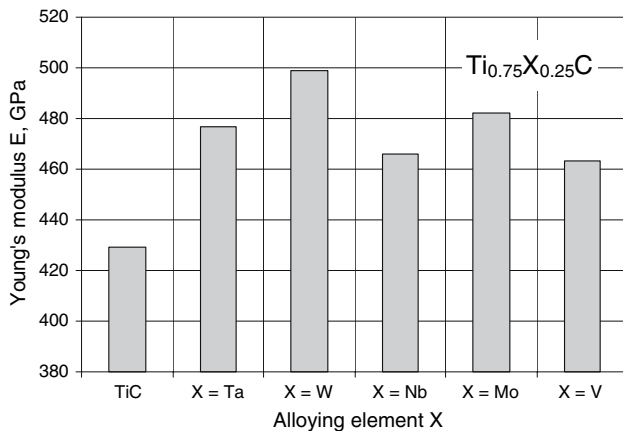


Fig. 3 The effect of alloying additions on the calculated Young's modulus for the $\text{Ti}_{0.75}\text{X}_{0.25}\text{C}$

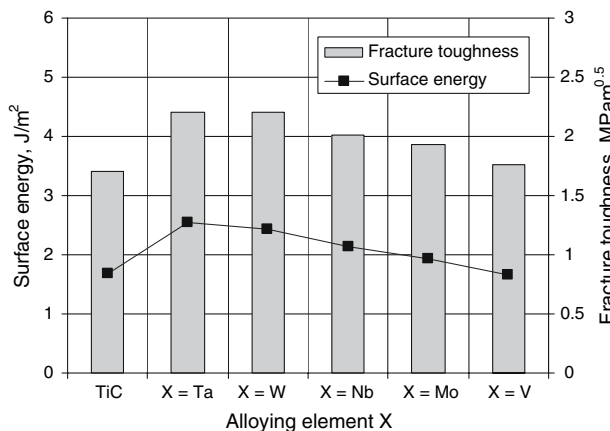


Fig. 4 The calculated surface energy γ (J/m^2) and fracture toughness K_c ($\text{MPa m}^{1/2}$) for the $\text{Ti}_{0.75}\text{X}_{0.25}\text{C}$ ceramics

the calculated fracture toughness K_{IC} from Eq. 10 together with the surface energy γ are plotted in Fig. 4. According to Fig. 4, all alloying additions except for vanadium increase surface energy γ , with tantalum achieving the best effect by $\sim 50\%$. It is also observed that both tantalum and tungsten increase the fracture toughness by $\sim 29\%$ compared to pure TiC. In addition, Fig. 4 also shows the trends of the calculated γ and K_{IC} for TiC and $\text{Ti}_{0.75}\text{X}_{0.25}\text{C}$. It is interesting to note that K_{IC} follows a similar trend as that of γ , indicating that surface energy γ plays a dominating role in determining the fracture toughness of these materials. In present calculations, only the (001) surface orientation was considered. However, in practical applications, the orientation of the coating surface may be different from the (001) direction. Therefore, DFT calculations for the case of (110) and (111) surface orientations are underway for $\text{Ti}_{0.75}\text{X}_{0.25}\text{C}$.

Conclusions

Young's modulus E and surface energy γ that determine the fracture toughness K_{IC} of TiC and $\text{Ti}_{0.75}\text{X}_{0.25}\text{C}$ ceramics ($X = \text{Ta}, \text{W}, \text{Mo}, \text{Nb}$ and V) were calculated using ab initio density functional theory calculations. Among alloying additions, tungsten achieves the best effect in increasing Young's modulus ($\sim 16\%$), while tantalum is the most effective in increasing the surface energy ($\sim 50\%$) of the $\text{Ti}_{0.75}\text{X}_{0.25}\text{C}$ system. Both Ta and W were the most effective in enhancing the fracture toughness K_{IC} of the TiC by $\sim 29\%$. Therefore, compared to pure TiC, both $\text{Ti}_{0.75}\text{Ta}_{0.25}\text{C}$ and $\text{Ti}_{0.75}\text{W}_{0.25}\text{C}$ may be better candidates for erosion-resistance coating applications.

Acknowledgement This work was performed thanks to the New Initiative Fund from the Institute for Aerospace Research of the National Research Council Canada.

References

1. Paramesvaran VR, Immarigeon JP, Nagy D (1992) Surf Coat Technol 52:251
2. Paramesvaran VR, Nagy D, Immarigeon JP, Chow D, Morphy D (1994) In: Koul AK, Paramesvaran VR, Immarigeon JP, Wallace W (eds) Advances in high temperature structural materials and protective coatings. Publication from National Research Council of Canada, Ottawa, pp 262–281
3. Tabakoff W (1999) Wear 233–235:200
4. Klein M, Simpson G (2004) In: Proc. ASME Turbo Expo 2004, Vienna, Austria, pp 1–6
5. Evans AG (1979) In: Preece CM (ed) Treatise on materials science and technology, vol 16 erosion. Academic Press, NY, pp 1–67
6. Ruff W, Wiederhorn SM (1979) In: Preece CM (ed) Treatise on materials science and technology, vol 16 erosion. Academic Press, NY, pp 69–126
7. Kresse G, Furthmuller J (1996) Comput Math Sci 6:15
8. Kresse G, Furthmuller J (1996) Phys Rev B 54:11169
9. Kresse G, Joubert J (1999) Phys Rev B 59:1758
10. Perdew JP, Chevary JA, Vosko SH, Jackson KA, Pederson MR, Singh DJ, Fiolhais C (1992) Phys Rev B 46:6671
11. Boettger JC (1994) Phys Rev B 49:16798
12. Ohring M (1992) The materials science of thin films. Academic Press, pp 568–570
13. Warren R (1978) Acta Metallurg 26:1759
14. Maerky C, Guillou M-O, Henshall JL, Hooper RM (1996) Mater Sci Eng A 209:329
15. Ahuja R, Eriksson O, Wills JM, Johansson B (1996) Phys Rev B 53:3072
16. Choy MM, Cook WR, Hearmon RFS, Jaffe H, Jerphagnon J, Kurtz SK, Liu T, Nelson DF (1979) In: Hellwege K-H, Hellwege AM (eds) Elastic, piezoelectric, pyroelectric, piezooptic, electro-optic constants and nonlinear dielectric susceptibilities of crystals. Springer-Verlag, Berlin
17. Dudiy SV, Lundqvist BI (2001) Phys Rev B 64:45403
18. Arya A, Carter EA (2003) J Chem Phys 118:8982
19. Haines J, Leger JM, Bocquillon G (2001) Annu Rev Mater Res 31:1